Observation of the Triplet Metastable State of Shallow Donor Pairs in AlN Crystals with a Negative-*U* Behavior: A High-Frequency EPR and ENDOR Study

Sergei B. Orlinskii[*] and Jan Schmidt

Huygens Laboratory, Leiden University, P.O. Box 9504 2300 RA Leiden, The Netherlands

Pavel G. Baranov[†]

Ioffe Physico-Technical Institute, St. Petersburg 194021, Russia

Matthias Bickermann, Boris M. Epelbaum, and Albrecht Winnacker

[1]*Department of Materials Science 6, University of Erlangen-Nrnberg, Martensstr. 7, 91058 Erlangen, Germany*
(Received 10 December 2007; published 24 June 2008)

Theoretical predictions about the *n*-type conductivity in nitride semiconductors are discussed in the light of results of a high-frequency EPR an ENDOR study. It is shown that two types of effective-mass-like, shallow donors with a delocalized wave function exist in unintentionally doped AlN. The experiments demonstrate how the transformation from a shallow donor to a deep (*DX*) center takes place and how the deep *DX* center can be reconverted into a shallow donor forming a spin triplet and singlet states.

PACS numbers: 71.55.Eq, 76.30.−v

Experimental and theoretical studies on the electronic properties of semiconductors have demonstrated that a donor can give rise to two types of electronic states. Either a shallow level with a delocalized effective-mass-like wave function associated with the normal substitutional site configuration, or a deep level with a localized wave function. The latter deep state is usually called a *DX* center and it arises from a lattice distortion at or near the donor site exhibiting a negative correlation energy *U* for electrons trapped at this site [1–3]. A transition of a shallow donor to a *DX*-like center is an important property that affects the *n*-type conductivity of semiconductors.

The formation of *DX* centers leads to a self-compensation of a shallow donor (SD) according to the reaction, $2d^0 = d^+ + DX^- + U$. Here, *d* denotes a substitutional SD impurity and *DX* the displaced deep impurity. The superscripts specify the charge state. In this model a SD can lower its energy by the capture of a second electron followed by a lattice relaxation of the donor impurity away from the substitutional site. The energy gain associated with electron pairing in the dangling bonds of a defect, coupled to a large lattice relaxation, was suggested by Anderson [4] to overcome the Coulombic repulsion of the two electrons.

The III–V nitrides could potentially be fabricated into optical devices that are active at wavelengths ranging from the infrared into the ultraviolet [5]. Unfortunately the properties of donors in the nitrides remain contradictory. While the authors of references [6,7] predicted that the *DX* state is the stable configuration for Si in AlN, Van de Walle [8] has argued that Si is a shallow effective-mass donor in AlN in contrast to oxygen that forms a *DX* center. Based on spectroscopically resolved photoconductivity and electron paramagnetic resonance (EPR) measurements, Si donors in heavily Si-doped MBE-grown AlN samples have been shown to exhibit a *DX*-like relaxation [9]. EPR and EPR-related methods have recently been used to deep-level defects in AlN [10,11], but to our knowledge there is no knowledge about the spatial distribution of the electronic wave function of shallow donors in the III–V nitrides and even more generally in the III–V semiconductors. Moreover the spin state of *DX* centers in semiconductors has not been demonstrated experimentally. High-frequency EPR and electron-nuclear double resonance (ENDOR) experiments were demonstrated [12,13] to be methods of choice for identification and study of effective-mass-like SD's in semiconductors.

In this letter we report the results of high-frequency EPR and ENDOR experiments on as-grown single crystals of AlN that prove the presence of effective-mass-like shallow donors in these crystals with a strongly delocalized electronic wave function. Secondly we demonstrate how the conversion of a shallow donor to an ionized shallow donor and a deep *DX*-like center and the reversed process take place.

The EPR and ENDOR experiments were performed at 1.5–5 K on a home-built spectrometer operating at 94.9 GHz (W-band) [14]. The spectra were recorded by monitoring the electron-spin echo (ESE) signal.

The crystal growth was accomplished by sublimation of the AlN charge placed in the hot zone of a tungsten crucible and subsequent condensation of the vapor species in a cooler region [15,16]. Two wurtzite polytype samples with dimensions of $0.3 \times 0.1 \times 0.3$ mm^3 labeled I and II were cut from larger boules of AlN grown with similar conditions.

Figure 1 shows the ESE-detected EPR spectra measured at 94.9 GHz in the two samples marked I (curve 1) and II (2,3) at 1.8 K after cooling from room temperature (RT) in the dark (1,2) and after 10 min light illumination (3). The
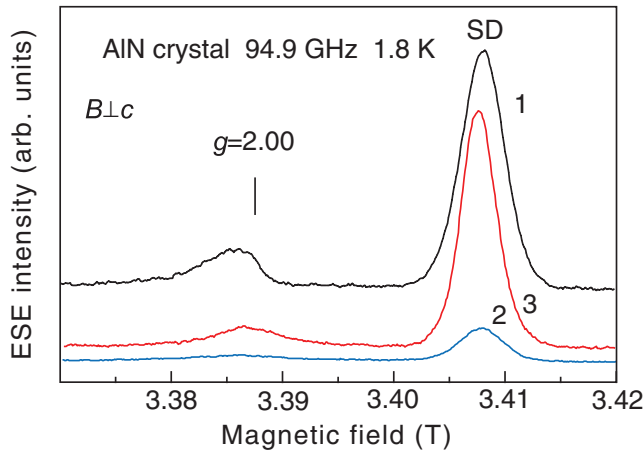
FIG. 1 (color). The EPR spectra of SD's for sample I (curve 1) and the sample II (2,3) at 1.8 K after cooling from room temperature in the dark (1,2) and after 10 min light illumination (3). The signal near $g = 2$ is thought to originate in a deep-level defect.

EPR signals were detected with the magnetic field perpendicular to the crystal c axis ($B \perp c$). The observed EPR signal at 3.408 T is characterized by a slightly anisotropic g factor of $g_{\parallel} = 1.9900$ and $g_{\perp} = 1.9894$. This g factor is somewhat smaller than the free electronic g factor as expected for SD's or conduction electrons in a wide-band-gap semiconductor such as AlN [9]. The anisotropy is consistent with the hexagonal symmetry of the AlN crystal. These factors support the assignment of the indicated resonances in Fig. 1 to SD's.

After cooling in the dark only a weak EPR signal of SD's is observed in sample II. After illumination with light with a wave length shorter then 700 nm, a strong EPR signal of SD's appears. This EPR signal, once excited at low temperature, persists at low temperature after switching off the light. The light-induced EPR signal of the SD's disappears after heating above 200 K. The EPR signal of the SD's in sample I did not increase upon optical illumination.

The EPR line of the SD's does not exhibit a resolved hyperfine (HF) structure and for this reason ENDOR spectroscopy at 95 GHz and at 1.5–2 K was performed. Figures 2(a) and 2(b) shows the ENDOR signal of ^{27}Al nuclei ($I = 5/2$, abundance 100%) observed in the EPR line (1) in sample I and the EPR lines (2,3) in sample II at 1.8 K. The ENDOR signals were measured in two orientations: $\theta = 54°$ (a) and $\theta = 90°$, $B \perp c$ (b). The nuclear Zeeman frequency of ^{27}Al is indicated by an arrow. For $S = 1/2$ the HF interaction constant a_i for each ^{27}Al nucleus i gives rise to two ENDOR transitions symmetrically placed around its nuclear Zeeman frequency when the quadrupole interaction (QI) is neglected. This symmetrical behavior is indeed observed for the "dark" SD signal although the HF lines are not resolved as in the case of SD in AgCl or ZnO [12,13]. In contrast, a considerable difference in intensity is observed for the ENDOR signals of light-induced SD's that are positioned in Figs. 2(a) and
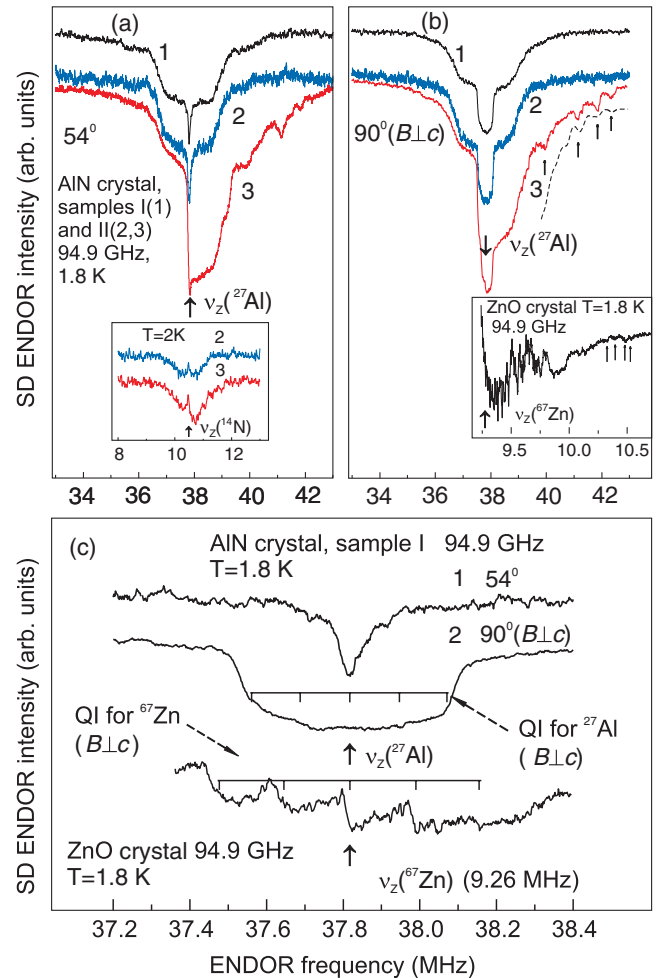

FIG. 2 (color). (a),(b) The ENDOR signal of ^{27}Al nuclei for samples I (1) and II (2,3) after cooling from RT in the dark (1,2) and after 10 min illumination (3); (a, inset) ENDOR signal of ^{14}N nuclei in sample II at 2 K; (b, inset) high-frequency part of the ENDOR spectrum of the SD's in ZnO crystal. (c) Central part of the SD ENDOR signal of ^{27}Al nuclei measured in sample I after cooling in the dark; (bottom) the SD ENDOR signals of ^{67}Zn nuclei in ZnO crystal.

2(b) above the nuclear Zeeman frequency of ^{27}Al and below this frequency. This difference in the intensities strongly depends on the temperature and increases when the temperature reduces. The ENDOR spectra consist of a multitude of lines which proved to be isotropic apart from a few lines in the Al spectrum which exhibit a small orientation dependence of the linewidth, and which are indicated by arrows in Fig. 2(b). These lines correspond to HF interaction constants a_i of 9.044, 7.994, 6.564, and 4.194 MHz. For comparison the inset in Fig. 2(b) shows the high-frequency part of the ENDOR spectrum of hydrogen SD's in ZnO single crystal with a resolved HF structure of ^{67}Zn nuclei [13]. The ENDOR spectra frequencies for AlN and ZnO were scaled proportionally to the ratio of their nuclear g factors. The similarity of both spectra supports the assignment of the EPR and ENDOR signals to SD's.

The ENDOR spectrum of the light-induced SD's shown in Figs. 2(a) and 2(b) can be understood by assuming that we are dealing with the triplet ground state of two exchange-coupled SD spins. The more intense signals above the nuclear Zeeman frequency of ^{27}Al are related to ENDOR transitions in the lower $M_S = -1$ sublevel, whereas the less intense signals below the nuclear Zeeman frequency correspond to the transition in the $M_S = 1$ sublevel. The intensities of the related ENDOR transitions differ strongly as a result of the extreme difference in the populations of the triplet sublevels at this low temperature and large Zeeman splitting. The ENDOR transition in the $M_S = -1$ sublevel will lie at a frequency $h^{-1}(1/2a_i)$ above or below the nuclear Zeeman frequency, depending on the sign of the HF constant a_i. From the observation that the intense group of lines that correspond to the transitions in the $M_S = -1$ level is positioned above the ^{27}Al Zeeman frequencies and the fact that the nuclear g factor for ^{27}Al has a positive sign, we derive that the HF interaction a_i has a positive sign, i.e., the SD induces a positive electron-spin density on Al nuclei.

A similar temperature dependent asymmetry is expected for the ^{14}N nuclear spins. This effect is indeed observed as shown in the inset of Fig. 2(a). Here the ENDOR signals of ^{14}N nuclei in sample II at 2 K are presented after cooling from room temperature in the dark (2) and after 10 min light illumination (3).

The central part of the ^{27}Al ENDOR spectrum measured in sample I after cooling from RT to 1.8 K in the dark is presented in Fig. 2(c) for the two orientations $\theta = 54°$ (1) and $\theta = 90°$ (2). The line width of the central part changes from 0.13 MHz for $\theta = 54°$ to 0.57 MHz for $\theta = 90°$. This broadening is caused by the quadrupole interaction. For comparison, the shallow donor ENDOR signals of ^{67}Zn nuclei observed in ZnO single crystals is presented as measured for $B \perp c$, and which reveal the QI. The quintet character of the lines in Fig. 2(c) is caused by the QI in remote Al shells ($I = 5/2$) for which the HF interaction is small. The ^{27}Al quadrupole splitting for $B \perp c$ is estimated to be ~ 0.135 MHz, therefore the intrinsic electric-field gradient at the Al sites about 1.5 times smaller than that for Zn sites in ZnO [17].

The strong intensity of the ENDOR line at the ^{27}Al Zeeman frequency is caused by a superposition of a large number of ENDOR lines with a very small HF interaction and supports the suggestion that the donor wave function spreads out considerably in space. In AlN the experimental value of the effective-mass $m^* = 0.33m_0$, the dielectric constant $\epsilon = 9.14$ and thus one expects that the effective Bohr radius of the $1s$-like envelope wave function $r_D \cong 1.5$ nm. This is almost the same value as for the SD in ZnO [13].

To identify the binding core of the SD's a search for ENDOR transitions of the nuclear spins of ^{29}Si, ^{13}C and ^{17}O was carried out. This search was unsuccessful probably due to the low natural abundance of these isotopes. Since the HF interactions with Al differ for the dark and

light-induced SD's an indication of the position of the binding core of these two types of SD's can be obtained from a simulation of the ENDOR spectra of the ^{27}Al nuclear spins similar to the case of the SD's in AgCl crystals [13]. To carry out this simulation we need to know the size of amplification factor, which relates the electron-spin density on nucleus i with the density of the envelope function of the SD. When putting the Coulombic center of the SD on a N site and assigning the largest observed ^{27}Al HF splitting of 9.04 MHz to the first Al shell we derive for the amplification factor a value $K_{Al} \sim 650$. When using this value we could derive a simulated ^{27}Al ENDOR spectrum as indicated by the dashed line in Fig. 2(b) which follows rather closely the experimentally observed ^{27}Al ENDOR spectrum. For this reason we believe that the Coulombic center of the light-induced SD is located on a N site and a possible candidate then might be O. A similar procedure for a SD with a Coulombic center at the Al site led to a much poorer fit of the simulated ^{27}Al spectrum to the experimentally observed one.

Pairs of the SD's having relatively strong isotropic exchange interaction J can be conveniently described in terms of the total spin, equal to 0 or 1. The corresponding singlet and triplet states are separated by J. To find J, the spin-lattice relaxation (SLR) rate was measured as a function of the temperature. The results are presented in Fig. 3(a) where the SLR rates $1/T_1$ are plotted as measured for the ESE signal of the SD's in sample II after cooling in the dark (filled circles) and after 10 min light illumination (open circles) with $B \perp c$ in the temperature range from 1.5 to 5 K. For the dark signal the SLR rate is independent of the temperature. For the light-induced signal the SLR rate is caused partly by an Orbach process [18], i.e., by a thermally induced excitation to and decay from a state that lies ~ 24 cm^{-1} above the lowest triplet state. We identify this higher lying state as the singlet state. The exchange interaction energy increases exponentially with decreasing separation between isolated donors. The distance of the two exchange-coupled donors can be estimated from the formula derived for the exchange interaction between two atoms in a hydrogen molecule which was modified in semiconductor crystals with regard to m^* and ϵ [19]. For the value J of 24 cm^{-1} the separation between coupled donors was found to be ~ 5.5 nm.

In Fig. 3(b), the energy-level diagrams for normal SD's ($S = 1/2$) and the light-induced SD's with DX behavior are shown. A schematic diagram of the positions of the singlet and triplet states of the SD pair coupled by an exchange interaction J as a function of the magnetic field are presented in the central part of Fig. 3(b). The Boltzmann distribution of the populations of the magnetic sublevels are indicated by different numbers of filled circles. It is not possible to resolve the two transitions (solid and dashed arrows) in EPR, however, they could be easily separated in the high-frequency ENDOR spectra. Figure 3(b) (right) shows a configuration-coordinate diagram for DX^- centers and shallow donor pairs d^0 coupled
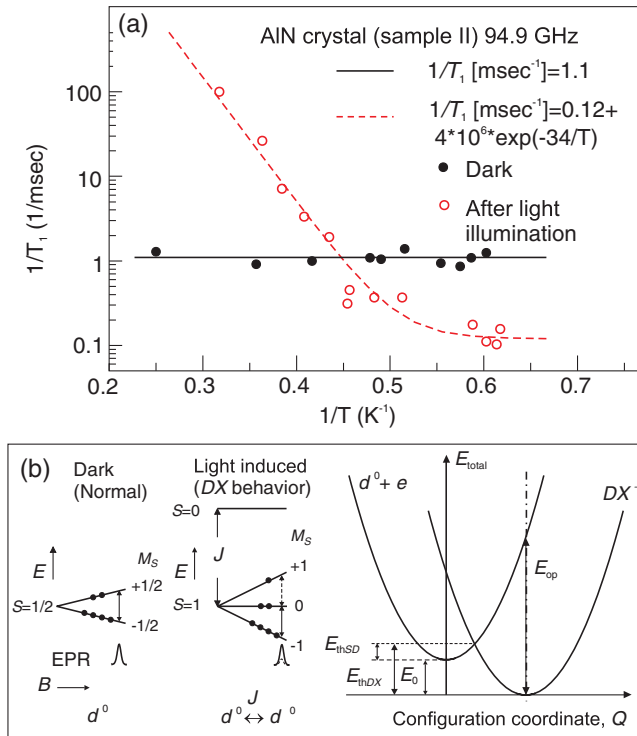
FIG. 3 (color). (a) The temperature dependence of SLR rate $1/T_1$ for ESE signal of SD's measured in sample II after cooling in the dark (filled circles) and after 10 min light illumination (open circles). (b) Energy levels diagrams for normal SD's measured after cooling in the dark ($S = 1/2$) and the light-induced SD pairs coupled by exchange interaction J with DX behavior. (right) Configuration-coordinate diagram for DX^- centers and SD pairs.

by an exchange interaction. The lower parabola represents the DX^- state. The illumination at low temperature transforms the stable d^+ and DX^- states into the meta-stable state of two SD's d^0 coupled by an exchange interaction. These d^0 states which represent the upper parabola generate the observed EPR signal of SD's with $S = 1$. The metastable state is separated from the d^+ and DX^- state by an energy barrier E_{thSD} which prevents the DX^- formation reaction to return back to the stable state. When the thermal energy is high enough to overcome the barrier E_{thSD} (~ 200 K) the EPR signal disappears. The striking result is the creation under the illumination in our experimental conditions of SD pairs with a well-defined exchange interaction.

In conclusion, two types of shallow, effective-mass-like donors have been observed in as-grown AlN crystals by EPR. The first type could be observed without illumination and is detected in a wide temperature range. The second type is only observed upon illumination with sub bandgap light at low temperatures and can be bleached after annealing at 200 K. The two types of shallow donors have similar EPR spectra and their shallow character is evident from the multitude of ^{27}Al ENDOR lines. The light-induced shallow donors correspond to coupled pairs with an exchange interaction of about 24 cm^{-1} and with a lowest triplet state. These pairs are believed to show a negative correlation energy U. Their Coulombic center is most probably located at the N position. For this reason we propose that oxygen forms the core of this donor. This proposal is in agreement with the theoretical prediction of Van de Walle [8] that oxygen in AlN undergoes DX formation.

*Also at Federal Center of Shared Facilities of Kazan State University, 42008 Kazan, Russia.
†pavel.baranov@mail.ioffe.ru

[1] G. A. Baraff, E. O. Kane, and M. Schluter, Phys. Rev. Lett. **43**, 956 (1979).
[2] G. D. Watkins and J. R. Troxell, Phys. Rev. Lett. **44**, 593 (1980).
[3] D. J. Chadi and K. J. Chang, Phys. Rev. Lett. **61**, 873 (1988).
[4] P. W. Anderson, Phys. Rev. Lett. **34**, 953 (1975).
[5] B. Monemar, P. P. Paskov, J. P. Bergman, A. A. Toropov, and T. V. Shubina, Phys. Status Solidi B **244**, 1759 (2007).
[6] C. H. Park and D. J. Chadi, Phys. Rev. B **55**, 12 995 (1997).
[7] P. Boguslawski and J. Bernholc, Phys. Rev. B **56**, 9496 (1997).
[8] C. G. Van de Walle, Phys. Rev. B **57**, R2033 (1998).
[9] M. W. Bayerl, M. S. Brandt, T. Graf, O. Ambacher, J. A. Majewski, M. Stutzmann, D. J. As, and K. Lischka, Phys. Rev. B **63**, 165204 (2001).
[10] P. M. Mason, H. Przybylinska, G. D. Watkins, W. J. Choyke, and G. A. Slack, Phys. Rev. B **59**, 1937 (1999).
[11] S. M. Evans, N. G. Giles, L. E. Halliburton, G. A. Slack, S. B. Schujman, and L. J. Schowalter, Appl. Phys. Lett. **88**, 062112 (2006).
[12] M. T. Bennebroek, O. G. Poluektov, A. J. Zakrzewski, P. G. Baranov., and J. Schmidt, Phys. Rev. Lett. **74**, 442 (1995).
[13] D. M. Hofmann, A. Hofstaetter, F. Leiter, H. Zhou, F. Henecker, B. K. Meyer, S. B. Orlinskii, J. Schmidt, and P. G. Baranov, Phys. Rev. Lett. **88**, 045504 (2002).
[14] J. A. J. M. Disselhorst, H. J. van der Meer, O. G. Poluektov, and J. Schmidt, J. Magn. Reson., Ser. A **115**, 183 (1995).
[15] B. M. Epelbaum, C. Seitz, A. Magerl, M. Bickermann, and A. Winnacker, J. Cryst. Growth **265**, 577 (2004).
[16] M. Bickermann, P. Heimann, and B. M. Epelbaum, Phys. Status Solidi C **3**, 1902 (2006).
[17] G. Denninger and D. Reiser, Phys. Rev. B **55**, 5073 (1997).
[18] A. Abragam and B. Bleaney, *Electron Paramagnetic Resonance of Transition Ions* (Oxford University Press, Oxford, 1970).
[19] E. Sonder and H. C. Schweinler, Phys. Rev. **117**, 1216 (1960).